Universidad de Valladolid

Escuela de Ingenierías Industriales

Grado en Ingeniería en Diseño Industrial
y Desarrollo del Producto

Development and Characterization of Plasma-Processed Graphite

Héctor Herrería Gil

Valladolid, Septiembre 2022

Título: Development and Characterization of Plasma-processed Graphite
Alumno: Héctor Herrería Gil
Fecha: Septiembre, 2022
Centro: Montanuniversität Leoben
Universidad: Universidad de Valladolid
Tutor: Eusebio de la Fuente

Eusebio de la Fuente

Montanuniversität Leoben

Valladolid, Septiembre 2022

Palabras Clave: Grafeno, Grafito, Plasma, Nanomateriales, Microporosidad

Resumen:

Hoy en día el grafeno es un material con grandes propiedades, usado por ejemplo en el almacenamiento de hidrógeno, gracias a su alta área superficial específica. El propósito de este trabajo es optimizar el proceso de exfoliación del grafeno y de la superficie funcional del mismo, mediante el uso únicamente de un sistema de plasma a baja presión. Con este procedimiento se comienza la investigación de los diferentes tratamientos posibles, utilizando en primer lugar Ar (argón) en el sistema, estudiando sus variaciones y caracterizándolo con técnicas como rayos-X para su estructura, espectroscopía Raman para más detalladamente cambios en la morfología y absorción/desorción de gas nitrógeno para evaluar su porosidad.

Affidavit:

I declare in lieu of ought, that I wrote this thesis and performed the associated research myself, using only literature cited in this work.

Leoben, September 2022	Héctor Herrería Gil

Index of abreviations

XRD	X-Ray Diffraction
PG	“Plasma Graphite”
REF	Reference Graphite
SA	Specific Surface Area
BET	Brunauer-Emmet-Teller
MFC	Mass Flow Controller
SCCM	Standard Cubic Centimeters per Minute

Acknowledgements

Without the help and collaboration of certain people, this study would have not been possible. I want to thank my supervisors Dr. Nikolaos Kostoglou and Prof. Christian Mitterer (Chair of Functional Materials and Materials Systems, Montanuniversität Leoben, Austria), for their support and for providing me with the opportunity to do my Bachelor thesis at the Chair of Functional Materials and Materials Systems, to Dr. Robert Franz for assisting me with the plasma activities, and to Dr. Christina Kainz for helping me with the Raman system.

Contents

1 Introduction

Nowadays exfoliated graphene appears in many research topic, due to its unique properties, graphene is the main choice to be used in the field of hydrogen storage including high surface area and ease of surface functionalization [1]. Graphene consists of a two-dimensional single-layer of sp^{2}-bonded carbon atoms. Few-layer graphene, composed of a limited number of stacked graphene layers, can be also produced in a porous form [2]. The production of nanoporous few-layer graphene-like materials, by using a plasma process technique, is one of the most common ways to achieve a high specific surface area, being the topic for considerable research [3][7].

Functionalized few-layer graphene shows enhanced chemical and thermal stability and can be further modified by different chemical reactions, including amidation, surface-initiated polymerization, and reduction of metal ions. This way a wide variety of objectives can be achieved due to its unique mechanical, optical, thermal and electronic properties [6].

The purpose for this bachelor thesis is to test and optimize the plasma system with the possibility of produce exfoliated graphene and surface-functionalized graphene avoiding wet processes. Therefore, there is a possibility to optimize the process for future research work related to plasma treatment, helping to achieve reliable graphene-like powders in a faster way. In order to overcome this challenge, the research starts with graphite powder provided by GBKB (Grafitbergbau Kaisersberg GmbH) and characterized previously at Montanuniversität Leoben [4]. The trials were compared with reference graphite sample from GBKB, to observe possible differences.

The materials were examined with various experimental techniques. These included X-ray diffraction (XRD), Raman spectroscopy analysis and nitrogen (N) ad-/desorption measurements at 77 K to characterize the morphological, structural and porosity properties.

2 Materials / Experimental Methods

2.1 Materials Description

Previous experiments showed the huge impact of the surface characteristics (morphology, porosity and chemistry) of powders on their surface behavior and properties [6]. Many physical properties of solids, such as density, thermal conductivity and mechanical strength, depend on their pore structure. Pores can be classified based on their size/width and shape. Based on their size, pores can be distinguished in three main types: macropores (width > 50 nm), mesopores (width 2-50 nm) and micropores (width < 2 nm) [2][5]. One sample of graphite is shown in Figure 2.1.

Fig.2.1 Reference graphite.

2.2 Characterization Methods

For studying crystal structure and characterizing the samples, XRD and Raman spectroscopy were used. Reference graphite XRD measurements were performed using a D8 Advance diffractometer (Figure 2.2) (Bruker-AXS, Karls-ruhe, Germany) equipped with Cu Kα radiation (λ ~1.54 Å) at 40 kV voltage and 40 mA current. Diffractograms were recorded using a continuous scan speed mode between the diffraction angles (2θ) of 10 ° and 90 °, a 0.01 ° step width and a 0.5 °/min scan speed. Based on recent research, the interlayer distance (d002) is in between the value for graphite-like carbon and turbostratic carbon [1] (turbostratic carbon is a special type of carbon in which graphene layers are not stacked in an ordered fashion, but relative rotations and translations between adjacent layers exist). No clear distinction can be made based on the diffraction pattern. Turbostratic carbon must not be confused with graphite. Turbos-

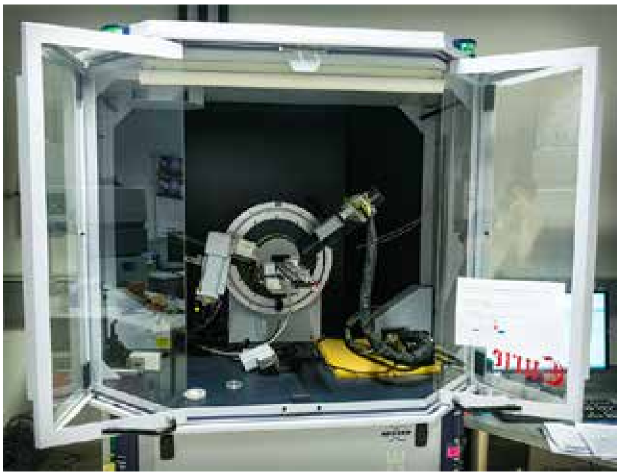

Fig. 2.2 Advance diffractometer.

tratic carbon features an increased interlayer distance compared to hexagonal graphite. Crystallographic parameters used to describe graphite carbons include the crystal length La which is the average crystal length in the a-direction of the unit cell, in-plane direction. Another parameter is the crystal length Lc which describes the average crystal length in the stacking direction. The interlayer distance d002 describes the average stacking distance between graphene sheets [4]. For reference graphite Lc is 13.8 nm, La between 7.9 and 11.9 nm, and interlayer distance d002 is 0.338 nm. A carbon crystallite structure drawing is in Figure 2.3.

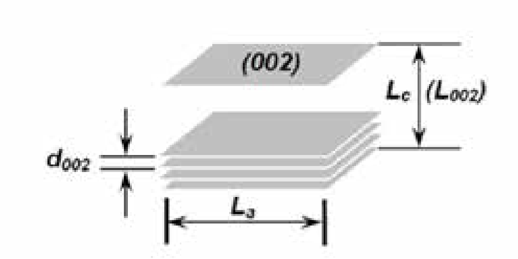

Fig. 2.3 Reference graphite crystallite sizes parameters.

Fig. 2.4 Witec spectrometer.

Raman spectroscopic studies were performed using an Witec spectrometer (Figure 2.4) and a solid-state laser emitting at 532.8 nm for excitation. Spectra were obtained from 500 cm^{-1} to 3500 cm^{-1} at room temperature, were used to analyze the microstructure of the material, in this case, to observe the peaks registered for every sample.

Gas sorption experiments were performed using a Quantachrome Autosorb iQ3 gas sorption analyzer from Anton Paar (Figure 2.5). Prior to the measurement all samples were degassed at 250 °C for 24 h under vacuum (10^{-6} mbar) in order to remove any physisorbed species from the surface of the materials. Samples of 1 g were placed in sample cells of 6 mm made of glass (Figure 2.6). This was done using nitrogen (N_2) as an adsorbate, recording all the samples at 77 K. The total specific surface area was calculated using the multi-point Brunauer-Emmet-Teller (BET) method at the lower relative pressure region ($0.12 < P/P_0 < 0.3$) of the adsorption data. It has to be noted that

Fig. 2.5 Gas sorption system.

the BET area is not equivalent to, but may be used as an estimate for the specific surface area, especially for the case of non-porous, macroporous, and mesoporous materials [3].

Fig. 2.6 6 mm cells used for powders.

2.3 Plasma Treatment

The main process in the investigation is the low pressure plasma treatment, using argon (Ar) inside the chamber of TETRA 30 (Figure 2.7). The system works with a power supply of 400 V. There are 4 gas channels controlled by 4 mass flow controllers (MFC), the system is totally controlled via PC (MS Windows). It has two different modes, manual or automatic operation, in which the parameters settings for a specific operation can be saved. Once the pressure is firstly then the Ar needed to fill the chamber is automatically applied by the system. The saturation of Ar was always 100 % of the maximum possible flow for each process, which was 250 sccm in all of the trials. The power of the electrode is a parameter that

Fig. 2.7 Plasma system.

de orientation has two options, an horizontal one with the possibility of using a rotational speed, and a vertical one placing the samples in a Petri dish without rotation. Two electrode options (shorter or larger) are also available in horizontal mode. Some of the elements are shown in Figure 2.8.

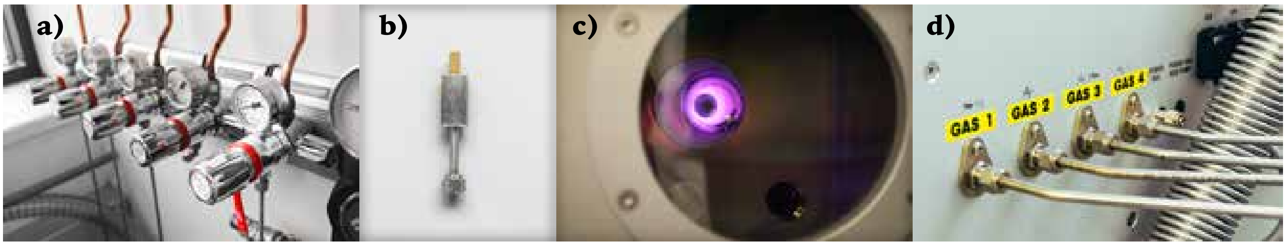

Fig. 2.8 individual components of the System: a) gas valves, b) short electrode, c) chamber and d) gas inputs.

3 Results and Discussion

The trials are realised in groups. 2 g of powder were used in each trial but just 1 g was placed into the plasma chamber, except for trial 1 which was 0.4 g and 1.6 g, as shown in Table 1. Furthermore, the preparation procedure was the same for every trial. First, the amount of the sample was placed into the recipient, using a small flask for PG15, a big flask and Petri dish for PG120-4. After plasma treatment the characterization process was done in this order: gas sorption, XRD, Raman for trial 1 and gas sorption and XRD for trials 2 and 3. Each trial parameters were power percentage, time during treatment, pressure inside the chamber, and rotation. Power percentage is the power supplied by plasma system. It was changed for each trial. Rotation was possible insidethe chamber when horizontal electrodes were used, the rotational speed of 50 % was selected for all the cases except for the second sample last trial. Last sample was treated using the flat electrode without rotation, also time and pressure were changed.

Table 1 Trials' process parameters.

		POWER	TIME	PRESSURE	ROTATION	WEIGHT
UNIT		(%)	(min)	(mbar)		(g)
TRIAL 1	PG 15	7	15	0.7	Yes	0,4
	PG 30	7	30	0.7	Yes	1,6
TRIAL 2	PG 120-1	25	120	0.4	Yes	1
	PG 120-2	25	120	0.1	Yes	1
TRIAL 3	PG 120-3	45	120	0.1	Yes	1
	PG 120-4	45	120	0.1	No	1

3.1 Trial 1

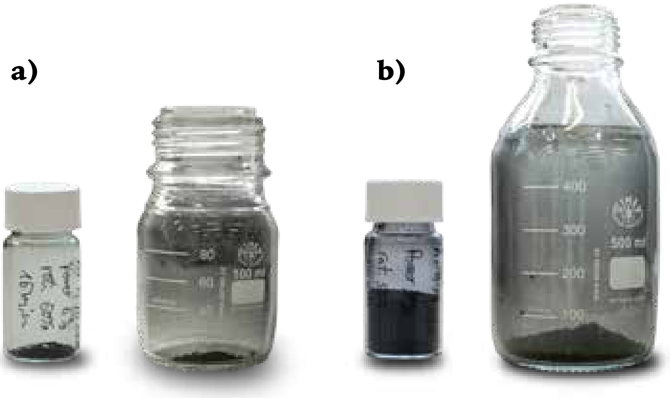

Fig. 3.1 a) PG15 sample and small flask of 100 ml, b) PG30 sample and big flask of 500 ml.

The samples used here were PG15 and PG30, as shown in Figure 3.1. They were treated for 15 and 30 min, respectively PG15 with a power of 7 % and a pressure value of 0.7 mbar. Rotational speed of 50 %, the main problem that occured with PG15 was that some of the powder was expelled from the bottle due to the pumping process inside the vacuum chamber. This problem was not easy to avoid for the next trials. It happened also with PG30 and with subsequent trials. After plasma treatment, gas sorption and desorption analysis are shown in Figure 3.2.

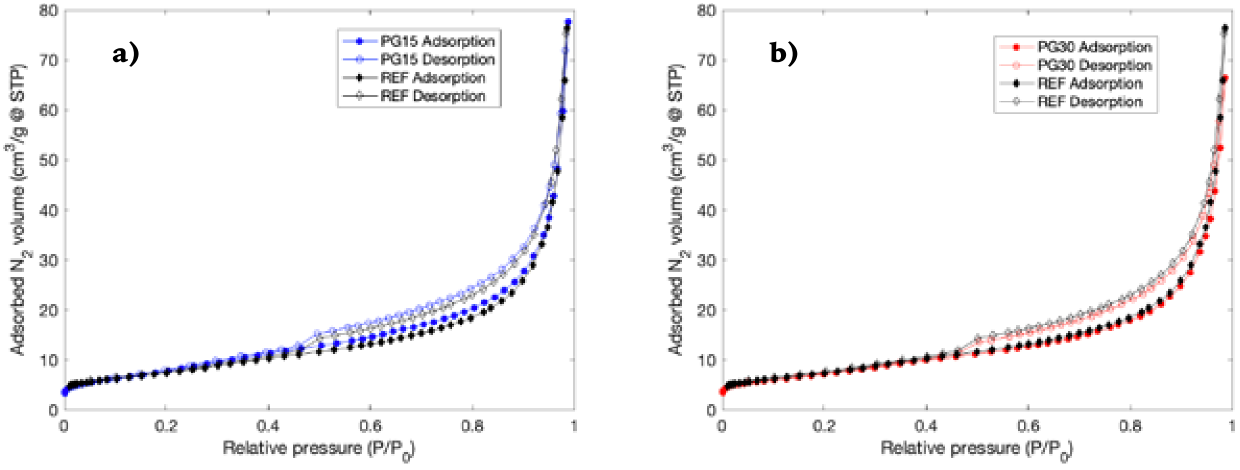

Fig. 3.2 Gas sorption comparison between a) REF and PG15 and b) REF and PG30.

Comparing REF with both samples, they present the same behavior. Both hysteresis loops are slightly shifted compared with REF. The appearance of a hysteresis loop indicates the presence of mesopores (pore widths 2-50 nm) within pore structure, related to the capillary condensation of N_2 gas inside the mesopores. No microporosity, observed (pore sizes < 2 nm). Also from BET, (Figure 3.3), is possible to extract the specific surface area (SA), which is the property that tells the relation between total surface area and solid mass. PG15 with 31 m^2/g and PG30 with 27 m^2/g present no big differences compared with REF (28 m^2/g). This could be due to low power and distance between electrode and powder. Samples were XRD characterized. In Figure 3.4 REF, PG15 and PG30 are shown. Similar structures, with some peaks to the (002) reflection from a graphitic phase at 26 °, and others less intense at 43 °, 54 ° and 77 °, (100)/(101), (004) and (110) crystal planes [4] .

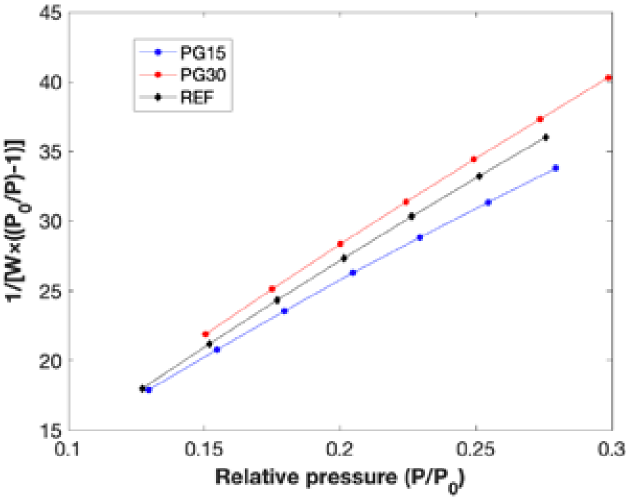

Fig. 3.3 PG15, PG30, and REF BET plotting comparison.

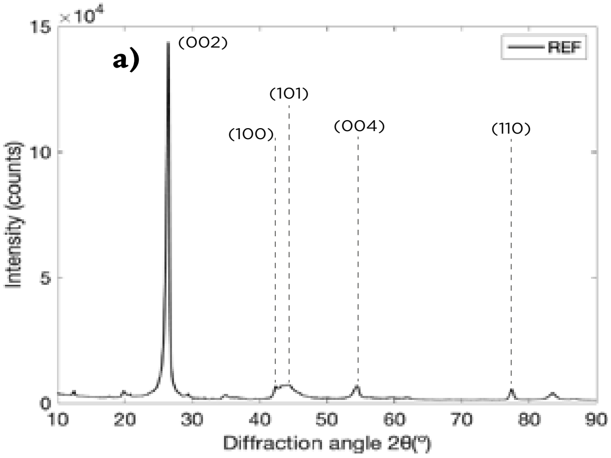

Raman spectra shown in Figure 3.5. As a qualitative description, the similarities between samples structure, D, G, and G'(2D) peaks are clearly visible. The presence of the 2D band indicates a certain degree of three-dimeensional order. Differences in Raman spectra indicate possible different microstructure [2].

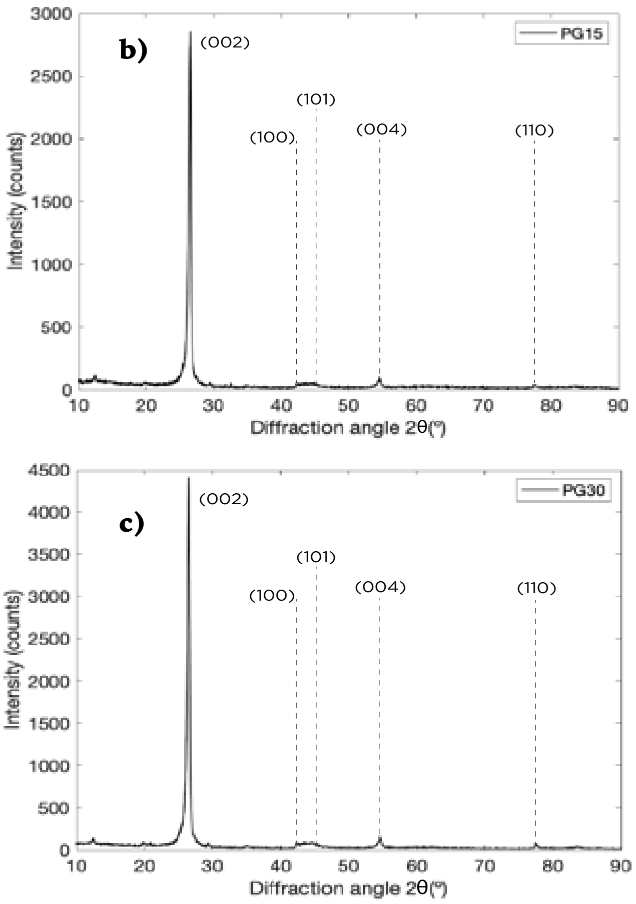

Fig. 3.4 X-ray diffractograms for a) REF, b) PG15 and c) PG30.

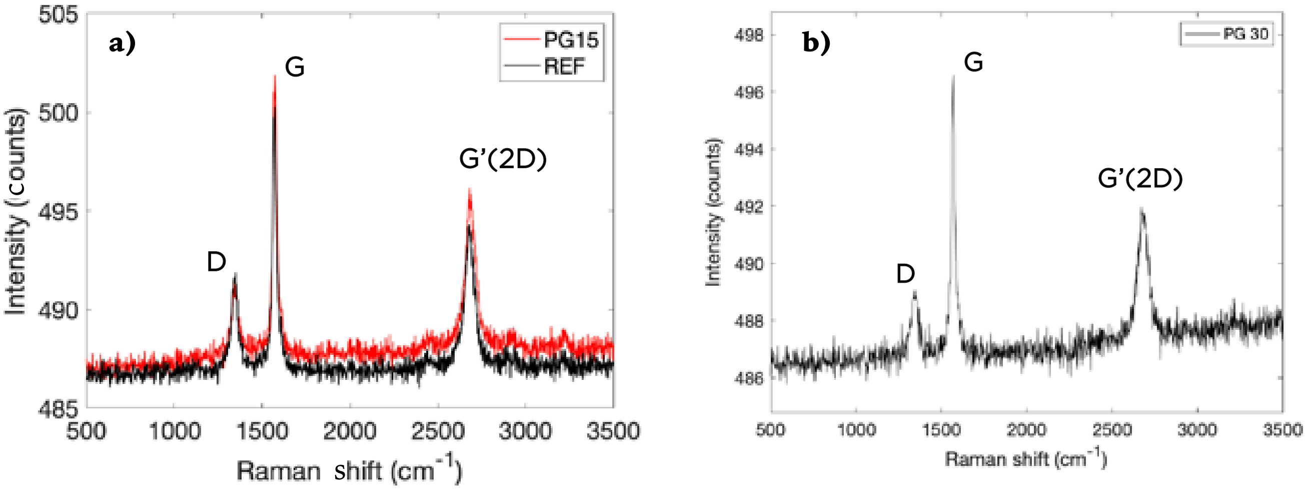

Fig. 3.5 a) comparison of Raman spectra between REF and PG15 and b) PG30.

3.2 Trial 2

First difference with trial 1 was the duration increase for 2 h for both samples (PG120-1 and PG120-2). The rotation power was set up to 50 %, plasma system power was 25 % and two different pressure settings, PG120-1 with 0.7 mbar and second one PG120-2, with 0.4 mbar, Figure 3.6 shows gas sorption comparison between a)PG120-1 and b)PG120-2 with REF, respectively. Hysteresis loops are similar in both cases. Possible causes are low power and the big distance between powder and electrode which was the same as in PG30. SA extracted from BET plotting between PG120-1, PG120-2, and REF is compared in Figure 3.7. They present similar values, 27 and 28 m^2/g respectively,

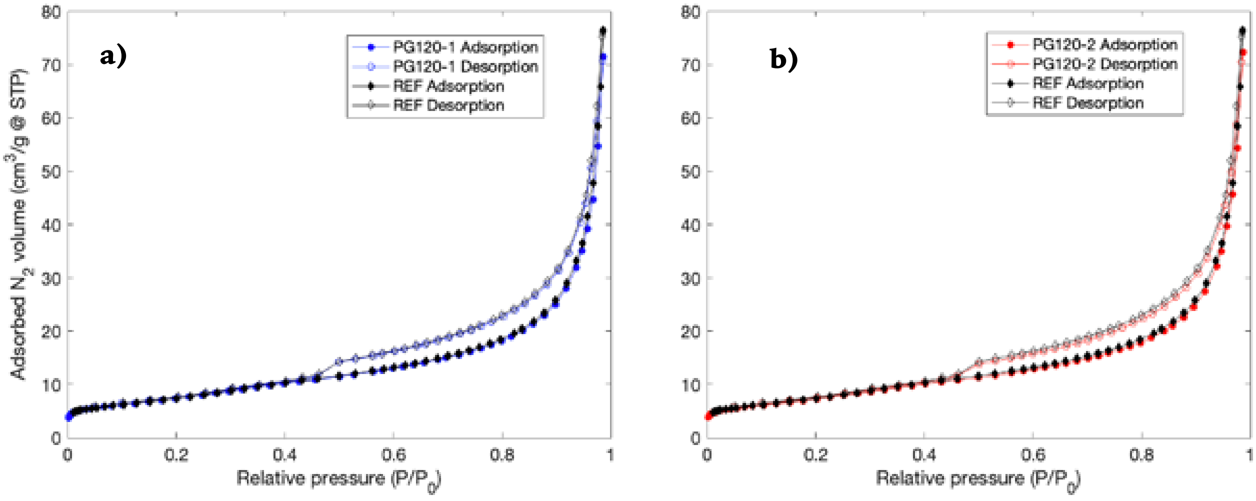

Fig. 3.6 gas sorption comparison between a) PG120-1 and REF and b) PG120-2 and REF.

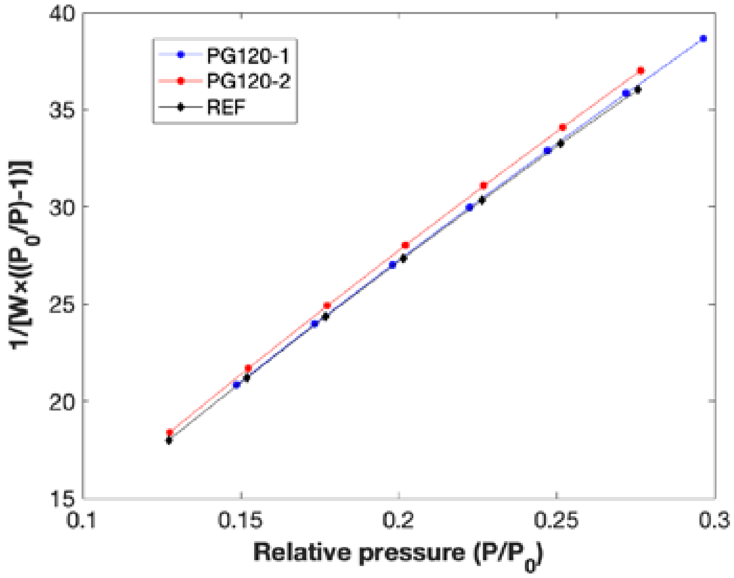

Fig. 3.7 PG120-1, PG120-2 and REF BET plotting comparison.

while REF was 28 m^2/g. Surface previous samples X-ray diffractograms can be observed in Figure 3.8, where PG120-1 and PG120-2 present same structures as previous samples and REF.

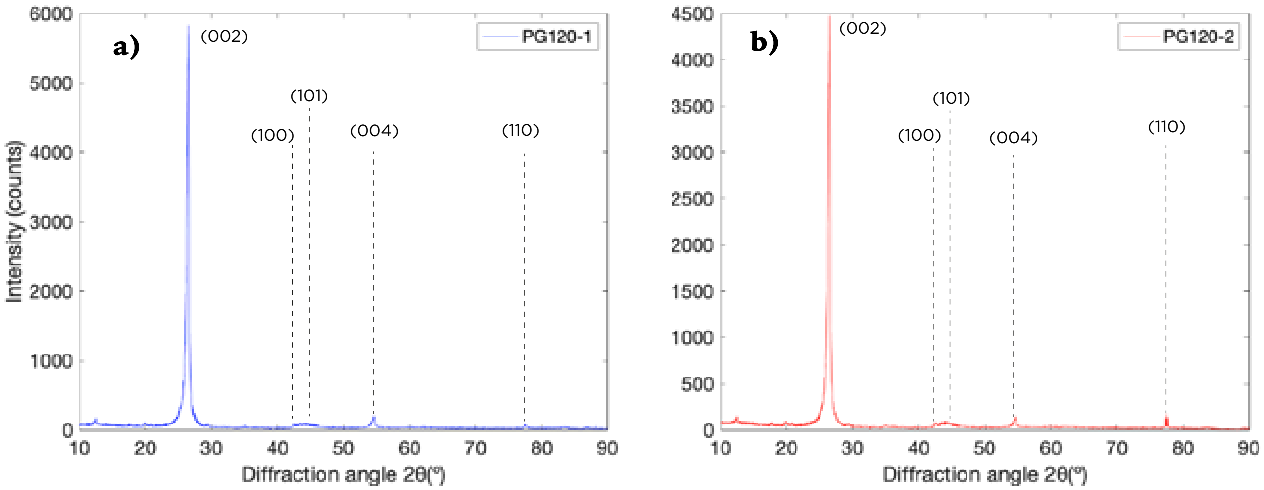

Fig. 3.8 X-ray diffractograms for a) PG120-1 and b) PG120-2.

3.4 Trial 3

The third trial was realised changing the power of the plasma system and the distance between the electrode and the surface. PG120-3 was treated with the horizontal to 45 %, chamber pressure at 0.1 mbar for 2 h. PG120-4 was treated using the flat electrode with no rotational speed option. This is closer to the previous samples but without rotation. Figure 3.9 shows both gas sorption comparisons, a) PG120-3 with REF and b) PG120-4 with REF, and c) BET plotting between REF and PG120-4.

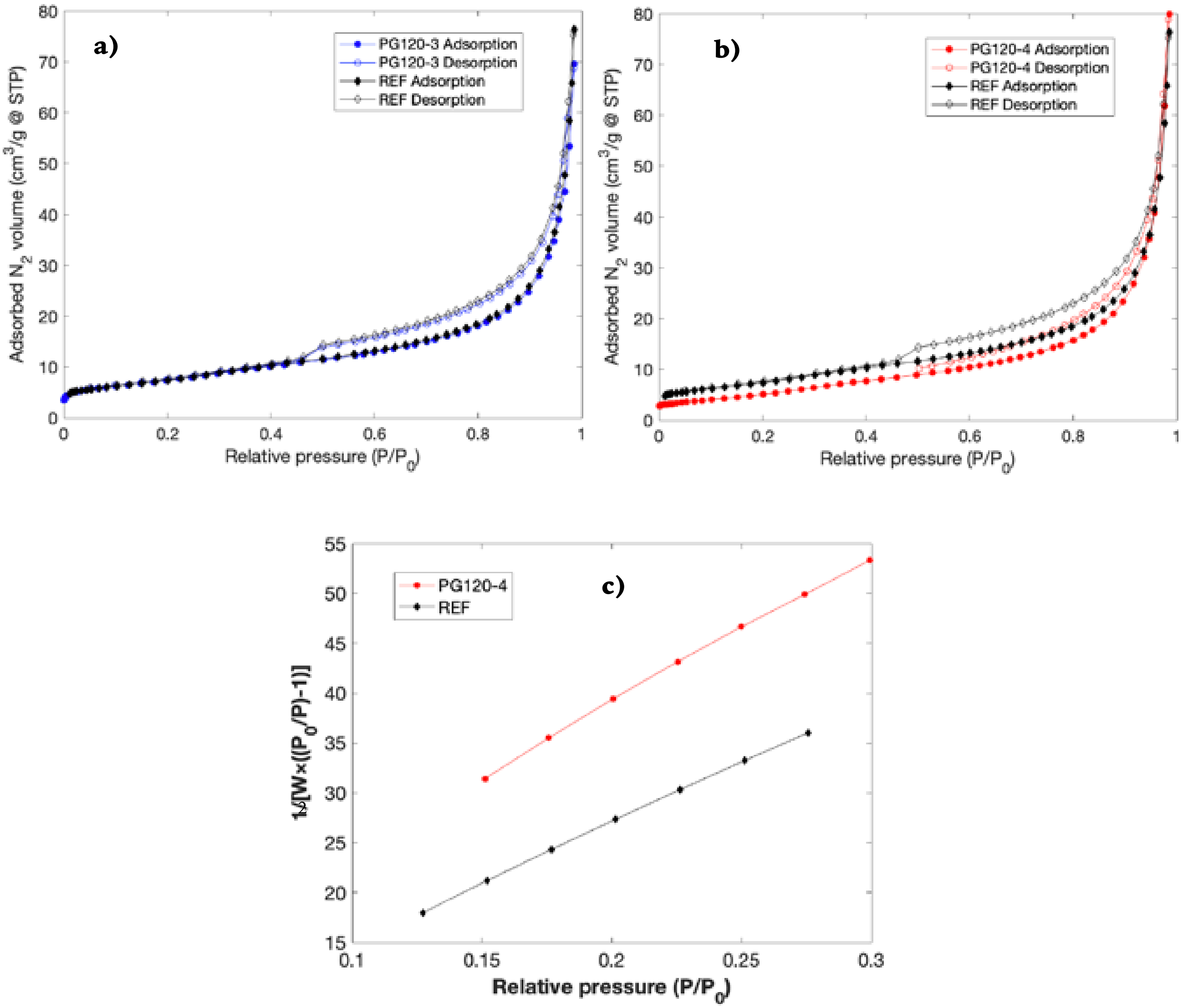

Fig. 3.9 a) PG120-3 and REF gas sorption comparison. b) PG120-4 and REF comparison. c) PG120-4 and REF BET comparison.

PG120-3 presents same hysteresis loop and same SA as REF with 28 m^2/g but PG120-4 has a slightly lower shifted hysteresis loop. This means the grain size has increased due to densification. PG120-4 SA is lower than the previous samples with 22 m^2/g. The closer distance between the sample and the electrode was the main change for having this densification. Figure 3.10 shows X-ray diffractograms for samples, where similar structures can be observed although PG120-4 presented a different gas sorption behavior.

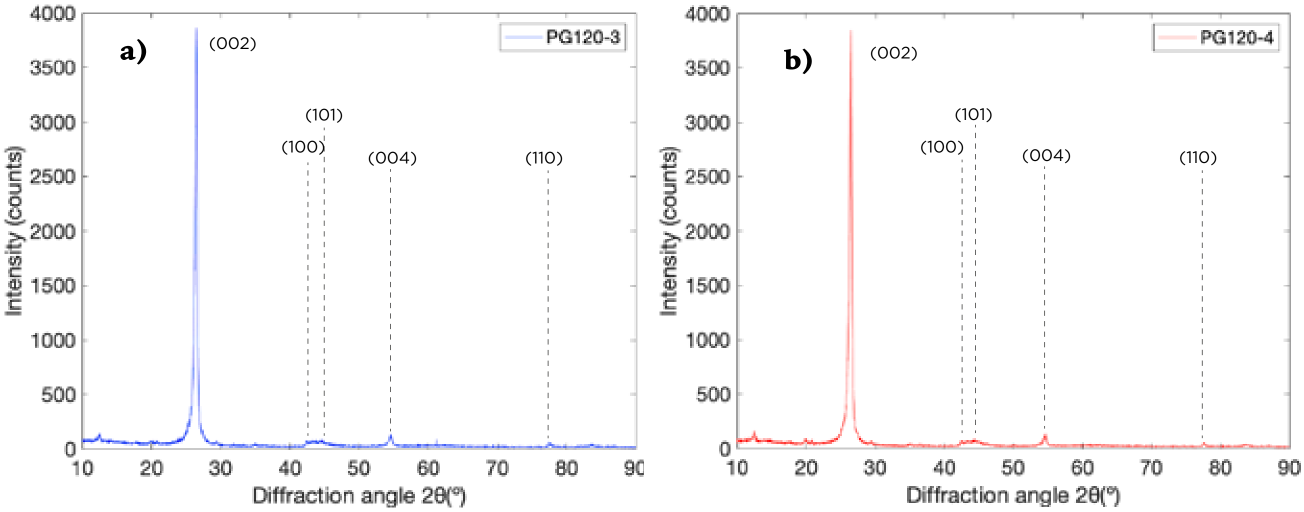

Fig. 3.10 X-ray diffractograms for a) PG120-3 and b) PG120-4.

4 Summary and Future Work

The results trials similar conclusions. One thing is the same for all and it is the crystalline structure, as X-ray diffractograms, where there are peaks to the (002) graphitic reflection, and others less intense (100)/(101), (004) and (110) crystal planes.Raman spectra for REF, PG15 and PG30 indicate that they have same crystal planes..

The N_2 adsorption/desorption isotherms recorded at 77 K present a small hysteresis loop related to capillary condensation of nitrogen within mesopores (pore widths 2-50 nm). There are no micropores (pore sizes < 2 nm). The only differences are the reduced adsorbed volumes for $P/P_0 < 0.95$ and the reduced surface area that both hint to a possible particle densification only for last sample, PG120-4, while the rest of the samples present same behavior as REF.

The parameters these trials refer to machine parameters, where there is still the possibility to increase the power of the plasma system (up to 90-100 %). The maximum power supplied was 45 %.

Different possible ways of continuing with the experiments are, for example, the use of other gases like N_2 , 0_2 , and H_2 . The findings of this thesis suggest that more information can be extracted from parameters such as longer times, changing flow and pressure values, and power of the plasma system. Future experiments will be based on conclusions from these experiments.

Bibliography

[1] N. Kostoglou, A. Tarat, I. Walters, V. Ryzhkov, C. Tampaxis, G. Charalambopoulou, T. Steriotis, C. Mitterer, and C. Rebholz, “Few-layer graphene-like flakes derived by plasma treatment: A potential material for hydrogen adsorption and storage,” Microporous and Mesoporous Materials, vol. 225, pp. 482–487, 2016.

[2] N. Kostoglou, “Carbon-based nanoporous materials for hydrogen storage”. PhD Thesis, Montanuniversität Leoben, Austria, 2017.

[3] N. Natter, N. Kostoglou, C. Koczwara, C. Tampaxis, T. Steriotis, R. Gupta, O. Paris, C. Rebholz and C. Mitterer, “Plasma-derived graphene-based materials for water purification and energy storage”.

[4] F. Knabl, “Structural Characterization of Carbons Derived from Methane Pyrolysis”. Master Thesis, Montanuniversität Leoben, Austria, 2021.

[5] M. Thommes, K. Kaneko, A. V. Neimark, J. P. Olivier, F. Rodriguez-Reinoso, J. Rouquerol, and K. S. Sing, “Physisorption of gases, with special reference to the evaluation of surface area and pore size distribution (technical report),” Pure and Applied Chemistry, vol. 87, no. 9-10, pp. 1051–1069, 2015.

[6] P. Goh and A. Ismail, “Graphene-based nanomaterial: The state-of-the-art material for cutting edge desalination technology”, Desalination, 2015.

[7] E. H. L. Falcao and F. Wudl. “Carbon allotropes: beyond graphite and diamond”. Journal of Chemical Technology & Biotechnology, Environmental & Clean Technology pp. 524–531, 2007. doi: https: //doi.org/10.1002/jctb.1693.

2